Biophysical Chemistry 154 (2011) 41–48

Contents lists available at ScienceDirect

Biophysical Chemistry

journal homepage: http://www.elsevier.com/locate/biophyschem

The conformational effect of para-substituted C8-arylguanine adducts on the B/Z-DNA equilibrium

Vorasit Vongsutilers [a,1], Daniel J. Phillips [b], Brian C. Train [a], Gregory R. McKelvey [a], Nissa M. Thomsen [a], Kevin H. Shaughnessy [c], James P. Lewis [d], Peter M. Gannett [a,*]

[a] Department of Pharmaceutical and Pharmacological Sciences, West Virginia University, P.O. Box 9530, Morgantown, WV, 26506, United States
[b] Department of Chemistry, Bethany College, Bethany, WV 26032, United States
[c] Department of Chemistry, The University of Alabama, Tuscaloosa, AL 35487, United States
[d] Department of Physics, West Virginia University, P.O. Box 6315, Morgantown, WV 26506, United States

ARTICLE INFO

Article history:
Received 7 November 2010
Received in revised form 19 December 2010
Accepted 19 December 2010
Available online 30 December 2010

Keywords:
B/Z DNA
Circular dichroism
Molecular dynamics
NMR
Nucleic acids
Thermodynamics

ABSTRACT

The B form of DNA exists in equilibrium with the Z form and is mainly affected by sequence, electrostatic interactions, and steric effects. C8-purine substitution shifts the equilibrium toward the Z form though how this interaction overcomes the unfavorable electrostatic interactions and decrease in stacking in the Z form has not been determined. Here, a series of C8-arylguanine derivatives, bearing a *para*-substituent were prepared and the B/Z equilibrium determined. B/Z ratios were measured by CD and conformational effects of the aryl substitution determined by NMR spectroscopy and molecular modeling. The *para*-substituent was found to have a significant effect on the B/Z DNA equilibrium caused by altering base-pair stacking of the B form and modifying the hydration/ion shell of the B form. A unique melting temperature versus salt concentration was observed and provides evidence relevant to the mechanism of B/Z conformational interconversion.

1. Introduction

The left handed form of DNA, Z DNA, was discovered thirty years ago [1] and several biological roles for this novel form of DNA have been discovered [2]. The formation of Z DNA has been implicated as a causative factor in genetic instability [3,4], mutagenesis [5], and carcinogenesis [6–8]. Several Z DNA binding proteins have been discovered including ADAR1 [9], E3L [10–12], and DML-1 [13] and have a variety of biological functions. Interestingly, this DNA conformation may play a protective role for certain viruses and consequently has been targeted for drug design [14].

Many factors that affect the position of the B/Z DNA equilibrium have been identified. The most significant is the requirement for alternating purine–pyrimidine sequence. Salt concentration plays an important role and high concentrations favor the Z form. In addition, multivalent cations [15] or a polycations [16] are more effective at driving the equilibrium toward the Z form. The main reason for the salt effect is Z DNA has a very narrow minor groove [17]. The localization of negative charge that results creates a very unfavorable electrostatic interaction that can be overcome by a high concentration of salt.

Certain steric effects are also important. Several base modifications are known to sterically drive the B/Z DNA equilibrium including C5-substituion of cytosine (e.g., C5-methylcytosine) [18] and C8 substitution of purines (e.g. C8-methyl). Remarkably, C8-bromination [19] or methylation [20,21] eliminates the need for high salt concentrations. Other C8 substituents have been studied with respect to the B/Z DNA equilibrium, including aminofluorene [22], 4-aminobiphenyl [23], and phenyl [24]. Invariably, all cases of C8-purine substitution of Z-prone sequences have been found to shift the equilibrium toward the Z DNA form, though to different degrees.

The shift caused by C8-purine substitution has been attributed to an unfavorable steric interaction between the C8 substituent and the H-2′ proton of the attached deoxyribose. In turn, this alters the preferred conformation about the glycosidic bond from *anti*, as found in B DNA, to *syn*, as found for purines in Z DNA. Consequently, C8-purine substitution has been said to stabilize the Z DNA form. However, there is little, if any, direct evidence that C8-purine substitution stabilizes Z DNA and some studies have contradicted this proposal [20]. Furthermore, it is not clear how C8-purine substitution can overcome the unfavorable electrostatics present in Z DNA, a major factor destabilizing the Z form.

Here, we report on a series of C8-arylguanine derivatives (Fig. 1) that bear substituents at the *para*-position of the aryl group. These

* Corresponding author. West Virginia University, School of Pharmacy, Basic Pharmaceutical Sciences, P.O. Box 9530, Morgantown, WV 26506-9530, United States. Tel.: +1 304 293 1480; fax: +1 304 203 2576.
E-mail addresses: Vorasit.v@chula.ac.th (V. Vongsutilers), pgannett@hsc.wvu.edu (P.M. Gannett).
[1] Current address: Faculty of Pharmaceutical Sciences, Chulalongkorn University, Phayathai Rd., Pathumwan, Bangkok 10330, Thailand.

0301-4622/$ – see front matter © 2010 Elsevier B.V. All rights reserved.
doi:10.1016/j.bpc.2010.12.006

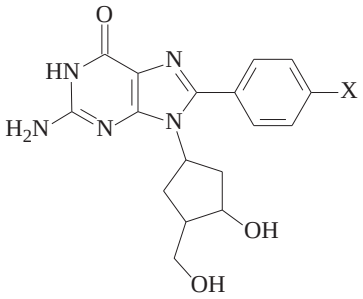

G^{8Ph} X = H G^{8MMPh} X = $-CH_2OCH_3$
G^{8Tol} X = $-CH_3$ G^{8CPh} X = -COOH
G^{8HMPh} X = $-CH_2OH$

Fig. 1. Structures of the five modified C8-arylguanines incorporated into to d $(CGCGCG^*CGCG)_2$ ($G^* = C^{8Ph}$, G^{8Tol}, G^{8HMPh}, G^{8MMPh}, and G^{8CPh}.

adducts form in DNA as a result of the metabolism of carcinogenic aryl hydrazines and related chemicals [25,26]. As Z DNA has been implicated in carcinogenesis, the effect arylation of guanine at the 8-position has on the B/Z DNA equilibrium may be related to arylhydrazine carcinogenesis. We have examined the simplest member of this group, C8-phenylguanine, in a CG decamer (CG^{8Ph}) [24,27]. This adduct significantly shifts the equilibrium toward the Z form. These studies suggested that the effect of the C8-phenylguanine modification on the B/Z equilibrium is multifaceted and generally due to destabilization of the B form and not stabilization of the Z form.

The studies reported here were designed to determine if the effect of the C8-arylguanine adduct on the B/Z equilibrium was general and to elucidate the effect of C8-purine substitution on both conformation and stability of the B or Z forms. In particular, C8-arylguanine containing oligonucleotides were prepared with variation of the *para*-substituent. The *para*-position is located such that substituents will, in the B form, interact with the phosphate backbone and locally alter stacking interactions of the aryl group, local geometry, and hydration. In addition, charged substituents should interact with the phosphodiester backbone with negatively charged substitutents reinforcing the steric effect of C8-purine substitution due to charge repulsion between the phosphate backbone and the substituent. To a large extent, these interactions will not occur in the Z form and shifts in the B/Z equilibrium toward the Z form should be driven by the *para*-substituent if destabilization of the B form drives the process. In contrast, if stabilization of the Z form is required, then the effect of the *para*-substituents should be to drive the B form toward single stranded DNA (ssDNA).

The *para*-substituent was found to have a remarkably significant effect on the B/Z DNA equilibrium. All derivatives studied were found to shift the equilibrium toward the Z form relative to the unmodified oligonucleotide. The salt dependence and thermodynamics values suggest that the arylated bases disrupt hydration. Molecular dynamics calculations and NMR studies indicate that this disruption is likely due to both local and global changes in geometry of the B form and that arylation has a negligible effect on the conformation of the Z form. Consequently, the overriding factor affecting the position of the B/Z DNA equilibrium is the extent of B DNA destabilization. Finally, a unique effect of salt concentration on melting temperature was observed for the oligonucleotides studied and supports the mechanism for B/Z interconversion proposed by Ha, et.al. [28].

2. Materials and methods

2.1. Materials

All chemicals used were purchased from Aldrich (Milwaukee, WI) unless otherwise noted. DNA synthesizer reagents and CPG columns were purchased from Glen Research (Sterling, VA). Anhydrous acetonitrile used in DNA synthesis was purchased from VWR (West Chester, PA). Anion exchange columns (DEAE-5PW) were purchased from Tosoh Bioscience (Montgomeryville, PA). NMR spectra were obtained on either a Varian 300 or a 600 spectrometer (Palo Alto, CA). ESI–MS, measured in negative ion mode, were recorded on a Finnigan LCQdeca (Waltham, MA). UV spectra were obtained on a Beckman DU640 spectrophotometer (Somerset, NJ). CD spectra were measured using a Jasco J-810 spectropolarimeter (Easton, MD). The oligonucleotides CG and CG^{8Ph} were prepared as previously described [24] as were the protected 8-(4-aryl)-2'-deoxyguanosine phosphoramidites needed for oligonucleotide synthesis [29].

2.2. Oligonucleotide synthesis

The oligonucleotides 5′CGCGCG*CGCG3′ ($G^* = G^{8Ph}$, (CG^{8Ph}) G^{8Tol} (CG^{8Tol}), G^{8HMPh} (CG^{8HMPh}), G^{8CPh} (CG^{8CPh})) (Fig. 1) were made on an ABI 394 DNA synthesizer through solid phase synthesis on 1 μmol scale. The syntheses utilized the standard protocol for automated DNA synthesis except for the C8-arylguanine modified phosphoramidites which were coupled by manual addition. The synthesized oligonucleotides were cleaved off the synthesis column and deprotected with ammonium hydroxide (30%, 55 °C, 20 h). The oligonucleotides were purified by FPLC using a gradient of 10 mM NaOH (A) and 10 mM NaOH/1 M NaCl (B) (gradient: 30–70% B over 60 min, flow rate: 6 mL/min, column: Tosoh TSK DEAE-5PW) and desalted with Waters Sep-Pack (C-18) cartridges.

2.3. Mass spectrometry

The purified CG decamers were examined by ESI–MS in the negative mode. Spectra were consistent with the desired products. Aqueous solutions of oligonucleotides (10 μM) were analyzed on a Finnigan LCQ deca using direct injection through a syringe pump (5 μl/min). The resulting series of m/z peaks, based on charge state (e.g., M^{6-}, M^{5-}, M^{4-}, and M^{3-}) of the oligonucleotides with different number of sodium adducts along with the calculated values are reported in Table S1.

2.4. CD analysis and molar fraction calculation

The oligonucleotide samples (25 μM) were prepared in phosphate buffer (10 mM, pH 7.4) and varying amounts of NaCl added to obtain a final concentration of 0–4000 mM NaCl. Before measuring spectra, oligonucleotide samples were annealed by heating to 90 °C and slowly cooling to room temperature. CD spectra of each sample were recorded at 10, 20, 30, 37, 50, 60, 70, 80, and 90 °C (220–350 nm, 50 nm/min). The molar fraction of B, Z and ssDNA were obtained as previously described [30]. The CD spectra were analyzed assuming that there is rapid equilibrium among three conformations (B DNA, Z DNA, and ssDNA) in solution. Therefore, at each temperature data were acquired, Eqs. (1) and (2) apply:

$$\Delta\epsilon^{295} = \Delta\epsilon_B^{295} * f_B + \Delta\epsilon_Z^{295} * f_Z + \Delta\epsilon_{ss}^{295} * f_{ss} \quad (1)$$

$$1 = f_B + f_Z + f_{ss} \quad (2)$$

where f is the mole fraction of one of the three possible oligonucleotide conformations and $\Delta\epsilon$ is the corresponding ellipticity of the oligonucleotide in that particular conformation. The $\Delta\epsilon$ values corresponding to each of the three possible conformations were estimated from the CD at a) low salt and at room temp ($\Delta\epsilon_B$), b) high salt and low temp ($\Delta\epsilon_Z$), and c) low salt and 90 °C ($\Delta\epsilon_{ss}$). An isosbestic point was observed at 270 nm corresponding to the case where Δ_ϵ for the B and Z forms are equal. Thus, f_{ss} could be determined applying

Eqs. (3) and (4) and then f_B and f_Z were solved from Eqs. (1), (2), and f_{ss}.

$$\Delta\epsilon^{270} = \Delta\varepsilon_{ds}^{270} * f_{ds} + \Delta\varepsilon_{ss}^{270} * f_{ss} \quad (3)$$

$$1 = f_{ds} + f_{ss} \quad (4)$$

2.5. Transition concentration

The transition concentration is the concentration of salt required such that the B/Z ratio is 1. This can be estimated by interpolation from the CD data and the ratios obtained by the methods described above. An alternative method to determine the transition salt concentration has been described and was also used here [31]. The basis of the approach is as follows. The effect of salt on the B/Z transition can be described as in Eq. (5):

$$B + c[NaCl] \overset{K_{eq}}{\rightleftharpoons} Z \quad (5)$$

where c[NaCl] represents the interactions of salt between the B and Z DNA conformations and c stands for the transition-specific constant coefficient. The observed equilibrium constant (K_{obs}) (calculated from f_Z/f_B), for a given salt concentration, is defined as shown by Eqs. (6) and (7):

$$K_{obs} = K_{eq} \cdot [NaCl]^c \quad (6)$$

$$ln(K_{obs}) = ln\left(K_{eq}\right) + c\ ln[NaCl] \quad (7)$$

Fitting a plot of $\ln(K_{obs})$ versus ln[NaCl] yields the values of c and K_{eq}, determined from the slope (c) and y-intercept ($\ln(K_{eq})$). In turn, the transition energy can be calculated from Eq. (8).

$$\Delta G_t = -RT\ ln\left(K_{eq}\right) \quad (8)$$

We note that the validity of Eq. (7) has been shown for salt concentrations above 0.9 M [32,33]. However, as shown in Table 1, the similarity of transition concentrations, determined by interpolation of the CD data or from plots of $\ln(K_{obs})$ versus ln[NaCl], are in good agreement and suggest that the relationship is valid at concentrations less than 0.9 M.

2.6. NMR analysis

The NMR samples (~0.8 mM in duplex) were made in phosphate buffer (10 mM, pD 7.4) without and with added NaCl (500 (CG^{8CPh}, CG^{8MMPh}, and CG^{8HMPh}) or 1000 mM (CG^{8Tol}) in D_2O and at 28 °C. Samples of the oligonucleotides, in the absence of NaCl, were mainly in the B DNA form while samples with NaCl (500 or 1000 mM) existed, predominantly, in the Z DNA form. The spectra obtained were used to assign the non-exchangeable protons of B and Z forms of CG^{8Tol}, CG^{8CPh}, CG^{8MMPh}, and CG^{8HMPh} (CG^{8Ph} spectra were previously reported [24]). The NOESY spectra of non-exchangeable protons were collected with a mixing time of 150 ms. The data was collected with 512 t_1 increments and 2048 t_2 complex points, each the sum of 16 transients. The COSY spectra were collected with 256 t_1 increments, each, the sum of 16 transients. The non-exchangeable proton assignment of B- and Z-DNA was conducted by following the sequential resonance assignment as previously reported [34–36].

Table 1
Transition concentration, transition free energy and thermodynamic parameters for B–Z transition of the unmodified and modified CG decamers.

Oligonucleotide	Transition conc. (mM NaCl)[a]	ΔG_t[b]	ΔG[c]	ΔH[c]	ΔS[c]
CG	3180	14.4 (1.0)	2.74	−10.6 (0.5)	−44.8 (2.8)
CG^{8Tol}	926	9.1 (0.8)	−0.33	−29.9 (1.9)	−99.3 (6.0)
CG^{8HMPh}	710	9.5 (0.8)	−0.80	−29.1 (1.8)	−94.9 (6.6)
CG^{8MMPh}	675	8.5 (0.6)	−0.73	−26.4 (2.1)	−86.2 (5.6)
CG^{8Ph}	585	7.0 (0.5)	−1.21	−32.4 (2.3)	−105 (8.4)
CG^{8CPh}	121	4.0 (0.4)	−1.99	−21.6 (1.3)	−65.6 (4.6)

[a] Determined from plots of $\ln(K_{obs})$ versus ln[NaCl] (mM). Similar values were determined by interpolation of the mole fraction data obtained by CD (see Materials and methods).
[b] Calculated for T = 310 K, $K_{B/Z} = 1$.
[c] Thermodynamic parameters were calculated from data obtained on solutions of oligonucleotides (25 μM) dissolved in phosphate buffer (10 mM, pH 7.4) and NaCl (500 mM NaCl) at 298 K (25 °C). ΔG, ΔG_t, and ΔH are in kcal mol^{-1}, ΔS is in cal mol^{-1} K^{-1}. Numbers in parenthesis correspond to the standard error.

2.7. Molecular modeling

Molecular dynamics was performed with Amber 10 [37,38]. Since atom parameters for C^8-arylguanine nucleosides were not available, these were developed. The modified base was built and optimized in Gaussian03 (Gaussian Incorporated, Wallingford, CT) at the HF 6–31 G* level, B3LYP basis set, to provide optimum bond lengths, angles, atom charges, and the torsional profile. These parameters where then adjusted for the Cornell 95 force field using the Amber programs nmode and resp, as we have previously described for the phenyl derivative [24,27].

Oligonucleotide structures were built in Sybyl (Tripos, Inc.) and transferred to Amber 10 [39]. The modified sequences studied here were CG^{8CPh} and CG^{8MMPh}. We have previously reported MD simulations of G^{8Ph}, G^{8Tol}, and CG^{8HMPh} [27]. The modified sequences were constructed from the unmodified sequence by attaching the appropriate aryl group to the C8-position of G6 and G16. Hydrogen atoms, sodium counter ions (to neutralize the charge), and a water box were added within xleap. Initially, the water and solute were equilibrated by minimizing the water and counterions with the DNA fixed (1000 steps) followed by 25 ps of non-particle mesh Ewald (PME) dynamics, raising the temp from 100 K to 300 K (DNA fixed), then 25 ps of PME dynamics to allow the water-counterion system to equilibrate, minimization (1000 steps) and then 3 ps of dynamics. This was followed by five consecutive 600-step minimizations, decreasing the harmonic potential from 20 to 0 kcal/mol in 5 kcal/mol steps. Production dynamics runs were then conducted for 4 ns with no constraints at 300 K.

The 'most representative' structure for each conformer was generated using the cluster trajectory option in the Dynamics Menu of MOIL-view [40]. Trajectories were split into 250 frame pieces using the ptraj module of Amber 10, necessary due to size limitations in MOIL-view for this particular trajectory analysis tool. The steps performed in the cluster analysis program were: (i) each frame is initially placed in a cluster by itself (ii) a cutoff distance of 2 Å specified, (iii) based on a 2D-RMSD matrix generated, the average RMSD between all pairs of structures for each pair of clusters was calculated (iv) the average RMSD for the most similar of these pairs is compared to the specified cutoff value and (v) if the value is less than the cutoff value, the two clusters are combined. This process is repeated until all cluster pairs have an average RMSD greater than the cutoff value. The 'most representative' structure of each cluster is that structure which has the lowest average RMSD to all other members of its cluster. Helical parameters of the most representative structures of the modified CG decamers were determined using CURVES [41,42].

3. Results

3.1. DNA synthesis

Oligonucleotides were prepared using standard protocols except that C8-arylguanine modified bases were coupled using manual

addition. This was required because when the C8-arylmodified guanine phosphoramidites were dissolved in acetonitrile a precipitate formed within 5–10 min that was insoluble in organic solvents. The nature of the precipitate is not known with certainty but we speculate that it may be related to the G-quartet. Guanosine and guanosine derivatives are known to form gels. Gel formation usually requires the presence of a metal cation though there is at least one report of a modified guanosine that forms a G-quartet in the absence of a metal cation [43].

After synthesis and FPLC purification, oligonucleotides were obtained in 30–40% yield (~89%/base). The relatively low oligonucleotide synthetic efficiency is likely due to the acid lability of the glycosidic bond of the C8-aryl modified bases and not to the use of manual coupling. We suspect that the trichloroacetic acid deprotection step may cause partial decomposition of the modified base during each coupling cycle. Finally, ESI–MS was used to aid confirming the structure of the synthesized oligonucleotides. The observed m/z ratios are in agreement with those calculated for the oligonucleotides prepared and both are shown in Table S1. Typically, the M^{3-}, M^{4-}, M^{5-}, and M^{6-} charge states were observed along with a range of sodium adducts.

3.2. CD based B/Z-DNA quantification

Representative CD spectra of the unmodified (CG) and the carboxyphenyl modified oligonucleotide (CG^{8CPh}), as a function of NaCl concentration (0–4000 mM), are shown in Fig. 2. CD spectra, as a function of salt concentration for CG^{8Ph}, CG^{8Tol}, CG^{8HMPh}, and CG^{8MMPh} are provided in the Supplementary information (Figs. S2–S5). The CD spectra of oligonucleotides in the B DNA form show peaks at approximately 220 nm and 280 nm and a trough at approximately 250 nm. In contrast, the CD spectra of the Z DNA form show a peak in the range of 260–270 nm and a trough at approximately 295 nm [44]. In agreement with previous studies of CG oligonucleotides [45], the unmodified CG decamer predominantly adopts the B conformation at salt concentrations below 3 M (at 37 °C), as indicated by the peak at 280 nm (Fig. 2a). Above 3 M NaCl, the peak at 280 nm is replaced by a trough at 295 nm that becomes more pronounced as the NaCl concentration is further increased. indicating that the Z DNA conformation was the predominate form present above ~3 M NaCl. The CD spectra of CG^{8CPh}, as a function of salt concentration, is shown in Fig. 2b. In this case the Z DNA conformation predominates at salt concentrations above approximately 125 mM (at 37 °C). Similar data was obtained with all modified oligonucleotides examined here, distinguished only by salt concentration at which the Z DNA form becomes predominant (Supplementary data, Figs. S2–S5).

The effect of the aryl guanine adduct on Z-DNA formation was quantitatively compared by determining the molar fractions of B, Z and ssDNA, as a function of salt concentration (0–4000 mM) and temperature (10–90 °C). Representative data for CG and CG^{8CPh} are shown in Fig. 3. Plotted in these figures are the mole fractions of the B, Z, and ssDNA forms of the oligonucleotide. Inspection of the plots for CG and CG^{8CPh} (see Supplementary data Figs. S6–S11) for complete temperature–salt concentration plots of CG, CG^{8CPh}, CG^{8Ph}, CG^{8HMPh}, and CG^{8MMPh}, indicates that, for duplexes, the B form shows the highest mole fraction at low salt and elevated temperatures. The mole

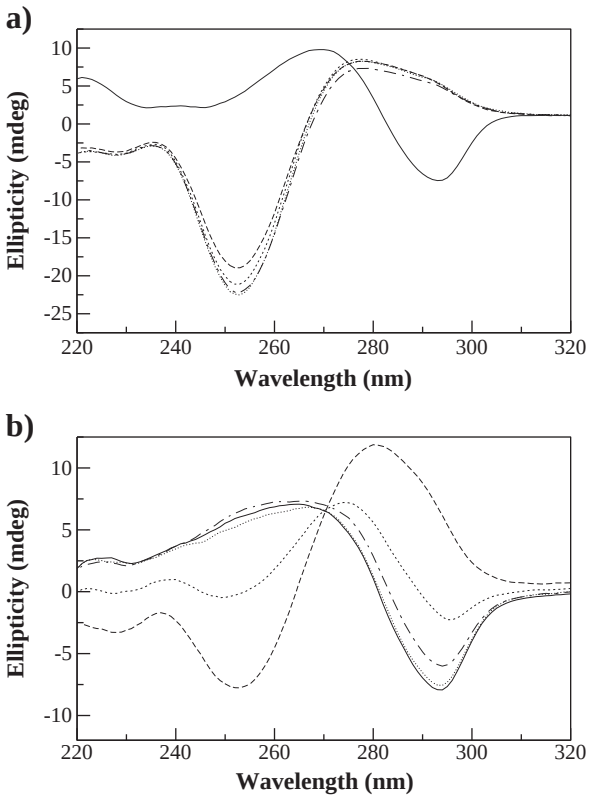

Fig. 2. CD spectra of a) CG and b) CG^{8CPh} at 0 (– – –), 100 (- - -), 500 (— - —), 1000 (•••), and 4000 (—) mM NaCl). All spectra were recorded at 37 °C in solutions containing approximately 25 μM of oligonucleotide and 10 mM phosphate buffer, pH 7.4.

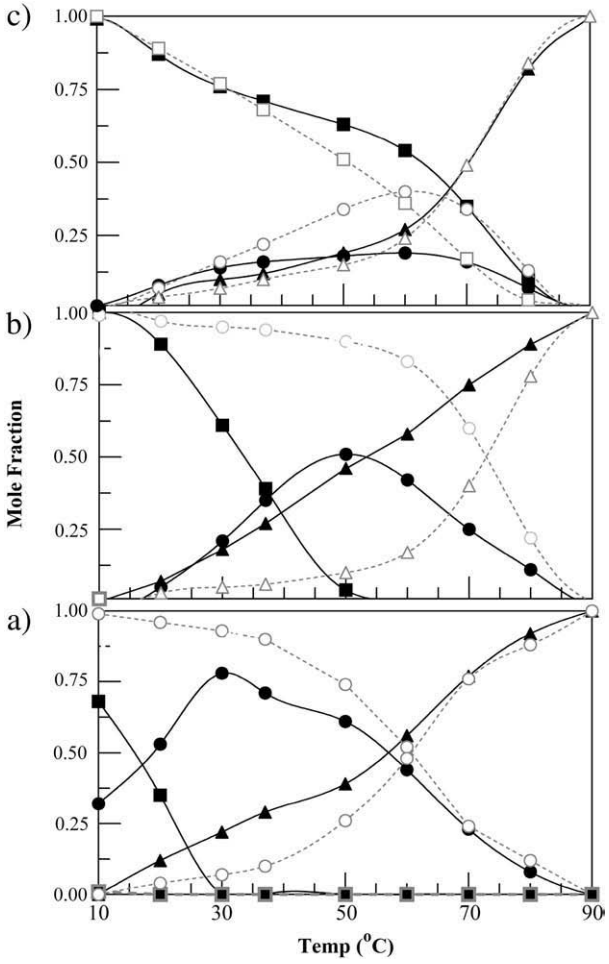

Fig. 3. Mole fractions of ssDNA (▲), B-DNA (●), and Z-DNA (■) of CG^{8CPh} and ssDNA (Δ), B-DNA (o), and Z-DNA (□) of CG, each at 25 μM, sodium phosphate buffer (10 mM, pH 7.4) and at selected salt concentrations including a) 0 mM NaCl, b) 100 mM NaCl, and c) 4 M NaCl. Solid and dashed lines were added to indicate the trends. Mole fractions were determined as describe in the Materials and methods section. Error bars have been omitted for clarity and the SE was less than 7% for all measurements.

fraction for the Z form shows just the opposite behavior and the ssDNA form increases with temperature.

3.3. Transition concentration and free energies

The mole fraction curves were used to estimate the transition concentration by interpolation of the mole fraction data at 37 °C and the estimated values are shown in Table 1. The transition concentration, as well as the ΔG_t, was also calculated by fitting $\ln(K_{B/Z})$ versus the salt concentration as described in the Materials and methods section. The resulting transition concentration and ΔG_t determined by this process are also listed in Table 1.

The CD data was also used to calculate the thermodynamic parameters for the B/Z-DNA equilibrium of the oligonucleotides studied here (Table 1). The data were calculated at a sodium chloride concentration of 500 mM and at 25 °C. This salt concentration was selected as it is the only one at which there were, for all the oligonucleotides studied here, measurable amounts of both the B and Z DNA conformers over the temperature range of 10–90 °C. The thermodynamic data were determined from the corresponding van't Hoff plots (Fig. S12).

3.4. Melting temperature and salt concentration

The curves depicting the distribution of mole fractions of the ss, B, and Z DNA forms, as a function of temperature at various salt concentrations, suggested that there was a significant dependence of T_M on salt concentrations. Consequently, the T_M was determined at the same salt concentrations as were the mole faction measurements. The data obtained were then plotted and are shown in Fig. 4. The data for the unmodified CG decamer is what is expected and as the salt concentration is raised from ~0 to 500 mM NaCl T_M, initially, increases rapidly, and then more slowly and is due to the binding of cations to the phosphate backbone [46,47]. Above ~500 mM NaCl, the T_M is seen to gradually decrease which has been ascribed to association of cations with the solvent over the solute leading to partial dehydration of the solute. In contrast, the behavior of the modified oligonucleotides is distinctly different. While all of the aryl modified oligonucleotides show an initial increase in T_M (<~25 mM), there is then observed a decrease up to a salt concentration that roughly corresponds to the transition concentration. The T_M then, again, increases up to the highest salt concentration used though the variation in T_M is variable across the modified oligonucleotides.

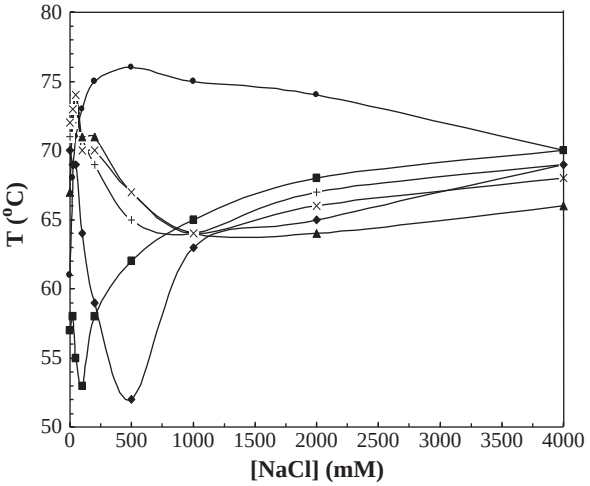

Fig. 4. The T_M of the unmodified (●), CG^{8Tol} (▲), CG^{8HMPh} (♦), CG^{8MMPh} (x), CG^{8Ph} (+), and CG^{8CPh} (■) decamer in phosphate buffer (10 mM, pH 7.4) at various NaCl concentrations (0–4000 mM). The data points corresponding to a given oligonucleotides are connected to emphasize the trends. Error bars have been omitted for clarity and the SE was less than 7% for all measurements.

3.5. NMR analysis

The NMR data were collected on each of the modified oligonucleotides at salt concentrations such that either the B or Z DNA form predominated. Since high salt concentrations cause line broadening, the lowest possible salt concentrations were selected for NMR measurements of the Z DNA form. Satisfactory data were obtained for the CG^{8CPh}, CG^{8MMPh}, and CG^{8HMPh} oligonucleotides at 500 mM NaCl and the CG^{8Tol} and CG^{8Ph} oligonucleotides at 1000 mM NaCl. Evidence for the presence of the Z DNA conformation was made by observing nOes between G-H1′ and G-H8 (at unmodified positions) in which the guanine bases adopt the *syn* conformation [35,36]. At low salt concentrations, these nOes were generally weak or unobservable [34], depending on the specific modification. Consequently, generally, it was not possible to obtain spectra of one isomer without the presence of the other and NMR derived structures were not generated. Proton assignments, COSY, and NOESY spectra of the modified oligonucleotides are given in Tables S2–S6.

The chemical shifts of C8-aryl protons could be assigned to the corresponding form. At low salt concentrations (B form) they were all upfield shifted relative to the free nucleosides (Table 2) or the corresponding protons in the Z form. This is likely due to shielding of the protons by the 5′-cytosine [24]. The effect is differential and the protons *ortho* to the purine ring shifted upfield (>1 ppm) by a greater amount relative to those that are *meta* to the purine ring. The spectra of the oligonucleotides in the B form also indicated that there is restricted rotation about the C8-aryl ring bond as the upfield resonances are broadened, relative to the downfield resonances. The broadening increases as the temperature is lowered and it decreases upon raising the temperature (data not shown).

3.6. Molecular modeling

Molecular modeling studies were conducted on CG^{8CPh} and CG^{8MMPh} as previously described for the remaining oligonucleotides studied here [27]. Since molecular dynamics yields a large number of structures, the most representative structure was selected from each trajectory for comparisons (see Materials and methods) [40]. Each of these structures was analyzed with CURVES to obtain the helicoidal parameters and groove widths. The results are compiled in Table 3 (B DNA only). Only the most significant results of the new simulations (CG^{8MMPh} and CG^{8CPh}) and CG oligonucleotide are shown. CURVES data for the remaining oligonucleotides can be found in the Supplementary data (Tables S7–S10). The backbone angles are not

Table 2
Chemical shifts of the G6-aryl protons of the aryl modified CG decamers in the B and Z conformation.

Oligonucleotide	Chemical shifts of G6-Ar protons (ppm)		
	Nucleoside[a]	B-DNA[b]	Z-DNA[c]
CG^{8Tol}	7.34, 7.53	6.28, 6.86	7.64, 7.69
CG^{8HMPh}	7.46, 7.62[d]	6.37, 7.10	7.73, 7.76
CG^{8MMPh}	7.47, 7.63	6.38, 7.07	7.74, 7.78
CG^{8Ph}	7.55, 7.64[e]	6.35/7.28, 7.04/7.32, 7.33	7.55, 7.65, 7.84
CG^{8CPh}	7.80, 8.07	6.72, 7.79	7.81, 8.16

[a] In dmso-d_6.
[b] All samples were in 10 mM phosphate buffer, pD 7.4 at 28°C.
[c] CG^{8Ph} and CG^{8Tol} spectra were measured on samples that were 1000 mM NaCl and 10 mM phosphate buffer, pD 7.4 at 28°C. CG^{8CPh}, CG^{8MMPh}, and CG^{8HMPh} samples were in 500 mM NaCl and 10 mM phosphate buffer, pD 7.4 at 28°C.
[d] As the TBS ether.
[e] Both resonances were multiplets, the downfield resonance integrated to two protons.

Table 3
Key helical parameters of the most representative structure for unmodified and modified oligonucleotides in the B DNA conformation.

	Inter-base pair					
	CG		CG^{8MMPh}		CG^{8CP}	
	C5-G6[a]	All BP[b]	C5-G6[a]	All BP[b]	C5-G6[a]	All BP[b]
SHF	0.81	0.06	−0.27	−0.13	−0.32	−0.01
SLD	−0.44	−0.14	−0.61	−0.06	−0.60	−0.01
RIS	3.00	3.18	3.60	3.40	3.37	3.31
TWT	32.2	31.5	28.8	32.0	34.1	31.8
	Base pair–helical axis					
	G6:C15[c]	All BP[b]	G6:C15[c]	All BP[b]	G6:C15[c]	All BPb
XDP	−2.22	−2.06	−0.79	−0.61	−1.06	−1.10
YDP	0.31	−0.17	−1.40	−1.57	−0.31	−0.20
INC	1.65	3.98	−2.35	−1.06	−1.57	0.39
	Groove width and depth[d]					
Groove	Width	Depth	Width	Depth	Width	Depth
Major	12.1	7.04	12.6	4.87	12.49	6.56
Minor	7.77	3.98	5.91	4.94	6.74	4.73

[a] Values reported are for the C5/G16-G6/C15 base pair step.
[b] Values reported are the average over all base pairs.
[c] Values reported are the average of both C5/G16 and G6/C15 base pair-axis values.
[d] Values reported correspond to the average taken over G4-C7/G14-C17.

provided in these tables as the values were within the ranges expected.

Both CG^{8MMPh} and CG^{8CPh} produce similar effects on the structure of the B forms as were observed for CG^{8Ph}, CG^{8Tol}, and CG^{8HMPh} [27]. At the modified base step, slide (SLD) and shift (SHF) for the G6–C15 (and the symmetry related C5–G16) base pair is more negative than the unmodified oligonucleotide. This is likely driven by a stacking interaction between the C8-aryl group of the modified guanine over the 5′-cytosine. Since the G6 (and G16) glycosidic bond is *anti*, the C8-aryl ring, to stack, has to twist in order to avoid clash with the H-2′ proton (purine-phenyl dihedral angle for MMPh = 20°, CPh = 23°). To accommodate the aryl ring twist and the *para*-substituent, there is an increase in rise (RIS) at the modified base. Locally, the helix is under wound for CG^{8MMPh}, as shown by the decrease in helical twist (TWT) as was observed for CG^{8Ph}, CG^{8Tol}, and CG^{8HMPh} [27]. Just the opposite was observed for CG^{8CPh}. The larger twist observed for CG^{8CPh} results in a greater separation of the negatively charged carboxylate and the phosphate between the 5′-cytosine and the modified base.

The base pair–axis parameters X-displacement (XDP) and Y-displacement (YDP), and inclination (INC) show modest changes relative to the unmodified oligonucleotide, similar to the differences previously reported for CG^{8Ph}, CG^{8Tol}, and CG^{8HMPh} [27]. Finally, the changes in the helical parameters noted, ultimately, produce changes in the widths of the major and minor grooves. Relative to the unmodified oligonucleotide, the major groove in the modified oligonucleotide (B form) increases in size, apparently to accommodate the aryl ring, while the minor groove width decreases.

Fig. 5 displays the G6/C7 base step for the CG, CG^{8MMPh}, and CG^{8CPh} oligonucleotides. The views presented were obtained by aligning the oligonucleotides on the sugar/phosphate residue connection between G6 and C7 (RMSd fit). The changes in the relative orientation between G6 and C7 caused by either the methoxyl methylphenyl (Fig. 5b) or carboxyl group (Fig. 5c) can be seen by comparison with the unmodified oligonucleotide (Fig. 5a). In particular, the differences in SLD and SHF cause G6 to be shifted toward the helical axis in the modified oligonucleotides. In turn, the C8-aromatic ring is drawn over C7 so that it stacks on C7. The twist of the aromatic ring attached to G6 is readily apparent (Fig. 5b,c). The difference in helical twist between CG^{8MMPh} and CG^{8CPh} can also be seen as the aromatic ring in CG^{8CPh} is nearer the G6 O5′ oxygen than it is in CG^{8MMPh}.

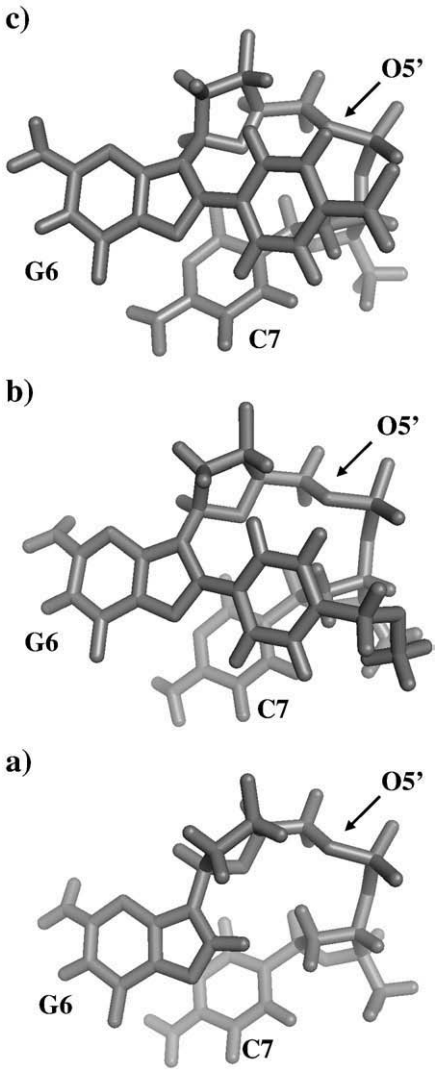

Fig. 5. Model of the G6/C7 base step for a) CG, b) CG^{8MMPh}, and c) CG^{8CPh}. See text for discussion.

Unlike the B forms, there were few significant differences observed in the helical parameters of the Z forms of the modified oligonucleotides relative to the unmodified oligonucleotide. There is variation in helical parameters (modified versus unmodified) but no systematic differences were observed with two exceptions. First, the CG steps are slightly over wound and, second, the minor groove has opened slightly, results that are similar to the previously reported results for CG^{8Ph}, CG^{8Tol}, and CG^{8HMPh} [27].

4. Discussion

There are a variety of known factors that cause the B/Z equilibrium to shift toward the Z form, including sequence, reduction of unfavorable electrostatic interactions, and steric effects such as those caused by substitution at the C5 position of cytosine or the C8 position of guanine. In addition, external factors such as salt identity, salt concentration, and temperature also affect the B/Z equilibrium. Consideration of these factors is often from the point of view of how they stabilize the Z form. However, changes in structure may destabilize the B form to such an extent that the Z form is adopted. Thus, it is not that, for example, the electrostatics of the Z form are especially bad rather that the B form (unmodified) is simply more stable than the Z form. Here, both steric and electrostatic effects on the B/Z equilibrium have been explored using experimental and computational methods. The oligonucleotides

used all bear a C8-*para*-substituted phenylguanine. The effect of this modification is to decrease the stability of the B form sterically, electronically, or both, while they have little effect on the stability of the Z form.

Experimentally, a measure of the effect that the *para* substituents examined here have on the B/Z equilibrium is the transition concentration (Table 1), the salt concentration required to cause the B/Z equilibrium to be equal to one. The unmodified oligonucleotide requires a salt concentration of approximately 3.2 M (at 37 °C). The introduction of aryl groups at the C8-guanine position lowers the transition concentration by a factor of ~3–25, depending upon the *para* substituent. The transition concentration was found to correlate with ΔG_t, the latter being a measure of the salt dependent component of the B/Z DNA equilibrium [31]. In particular, as the *para*-phenyl substituent was varied over the series $-CH_3$, $-CH_2OCH_3$, $-CH_2OH$, –H, $-CO_2^-$, the involvement of salt in the equilibrium decreased even though the equilibrium shifts toward the Z form.

In the present case, a plausible reason for this is that salt plays a decreasing role in stabilizing the B form as the *para*-substituent is varied. The decreased role of salt in stabilizing the B form could be due to a disruption in stacking caused by the *para* substituents (see below, molecular modeling) and/or disruption of the layer of hydration and associated ions. This theory is partially supported by the ΔS values reported for the unmodified and modified oligonucleotides as the entropy, for Z DNA formation, was found to be less favorable for the modified oligonucleotides than for the unmodified. Furthermore, the thermodynamic data for the B/Z equilibrium display enthalpy-entropy compensation. This compensation arises from the stabilizing effects of base-pairing and base-stacking and the associated unfavorable effects including the ordering of water or ions about the oligonucleotide [48]. In the present case, the modifications to the C8-position likely interfere with base-pairing, base-stacking or both, and enthalpically destabilize the B form but stabilized it entropically. In contrast, since the C8-aryl group lies outside of the Z DNA helix, it is unlikely that the C8-aryl modification interferes with pairing or stacking in the Z form, rendering this form stabilized with respect to enthalpy and destabilizing it, entropically, with respect to the B form.

The most representative structures obtained from molecular dynamics calculations are in agreement with the inferences made above. Both CG^{8MMPh} and CG^{8CPh} produce similar effects on the structure of the B forms as was observed for CG^{8Ph} [27]. The principle change that occurs by introduction of the aryl substituent is a repositioning of the base pair so that the phenyl portion stacks over the 5′-cytosine. The extent of the repositioning is dependent upon the *para* substituent, being the greatest for the phenyl group and less for the remaining derivatives. In turn, this shift, coupled with an increase in rise, work together to disrupt base-stacking, disrupt the solvation and ion network, and widen the major groove while narrowing the minor groove (B form). In contrast, there were few significant differences observed in the helical parameters of the modified oligonucleotides in the Z form relative to the unmodified oligonucleotide. The most significant differences are that the CG steps being slightly over wound and the minor groove has slightly opened. Overall, the molecular dynamics calculations suggest that the B form is destabilized due to decreased stacking and helical distortion at the site of the modified base.

As noted, in all cases examined, the phenyl ring stacks over the 5′-cytosine ring, albeit to varying degrees, and is completely contained within the helix (B form). In this geometry the aromatic protons should be shielded and upfield shifted relative to the free nucleoside or Z form. The NMR data (Table 2) bears out this prediction. The protons *ortho* to the purine ring are substantially upfield shifted in CG^{8CPh} and CG^{8MMPh} by 1.09 and 1.36 ppm, respectively, relative to the Z form in which the aryl rings cannot stack over the 5′-cytosine. Consequently, the NMR data agree with the molecular dynamics results and hence that the B form of the modified oligonucleotides is destabilized relative to the unmodified oligonucleotide.

At salt concentrations up to 25 mM, all of the oligonucleotides studied show an initial increase in T_M. Thereafter, the behavior of the unmodified and modified oligonucleotides diverges. The modified oligonucleotides show a decrease in T_M up to the transition concentration. Then, as the salt concentration is further increased, the T_M is observed to increase up to the highest salt concentration used. The variation in T_M (T_M (max) − T_M (min)) is greatest for the hydroxymethyl and carboxy derivatives, which vary 18 and 6 °C, respectively. The anomalous behavior may be explained in light of the mechanism for B/Z DNA interconversion, recently proposed by Ha, et.al., [28]. In this mechanism, the purine of a base pair, unpairs, rotates about the glycosidic bond such that it is no longer within the helix, rotates 180° about the plane of the purine ring system and the process reverses to reform the base pair but now in the Z conformation. Initially, as this process proceeds, base unstacking occurs along with the loss of a base pair. Both processes will destabilize the duplex and result in a decrease in T_M. This process will occur with the greatest frequency at salt concentrations that are at or are near the transition concentration and the greatest decreases in T_M should also occur at this point. In the case of the *para*-hydroxymethyl and *para*-carboxy derivatives, the larger variations in T_M near the transition concentration may be due to hydrogen bonding with water, causing greater resistance to restacking back into the helix.

In conclusion, C8-aryl substitution significantly alters the B/Z DNA equilibrium. The position of the equilibrium depends upon the substituent in the *para* position of the aryl group and the nature of the interaction between the substituent and the phosphate backbone. The position of the B/Z equilibrium, as modified by C8-arylguanine substitution, is driven mainly by destabilization of the B form, not stabilization of the Z form. The destabilization is not solely enthalpy driven, as entropy plays a significant role. We have also shown that the effect of C8 substitution is likely to be global and not simply a local effect. Thus, C8-guanine modifications may produce local steric interactions between the C8 substituent and H-2′ and the phosphate backbone, and other conformational changes that alter stacking and the major and minor groove widths, all of which affect the position of the B/Z equilibrium. Moreover, these effects can be modeled and make it possible to design C8-guanine substituents that will alter the B/Z DNA equilibrium in a predictable fashion. Being able to control the B/Z equilibrium may be useful for designing oligonucleotides to determine the mechanism of the B/Z conformational interconversion [28], the discovery of new Z DNA binding proteins [49], and to determine the mechanism whereby the binding of ZBP convert B DNA into Z DNA [50,51].

Acknowledgements

This work is funded in part through NSF Research Infrastructure Improvement Grants EPS 0554328 and EPS-1003907, and NIH for a fellowship to DJP (P20RR16477).

Appendix A. Supplementary data

Supplementary data to this article can be found online at doi:10.1016/j.bpc.2010.12.006.

References

[1] A.H.J. Wang, G.J. Quigley, F.J. Kolpak, J.L. Crawford, J.H. van Boom, G. van der Marel, A. Rich, Molecular structure of a left-handed double helical DNA fragment at atomic resolution, Nature 282 (1979) 680–686.
[2] A. Rich, S. Zhang, Z-DNA: the long road to biological function, Nat. Rev. Genet. 4 (2003) 566–573.
[3] G. Wang, L.A. Christensen, K.M. Vasques, Z-DNA-forming sequences generate large-scale deletions in mammalian cells, Proc. Natl Acad. Sci. USA 103 (2006) 2677–2682.

[4] J.R. Spitzner, I.K. Chung, M.T. Muller, Eukaryotic topoisomerase II preferentially cleaves alternating purine–pyrimidine repeats, Nucleic Acids Res. 18 (1990) 1–11.
[5] A.-M. Freund, M. Bichara, R.P.P. Fuchs, Z-DNA-forming sequences are spontaneous deletion hot spots, Proc. Natl Acad. Sci. USA 86 (1989) 7465–7469.
[6] R. Liu, H. Liu, X. Chen, M. Kirby, P.O. Brown, K. Zhao, Regulation of CSF1 promoter by the SWI/SNF-like BAF complex, Cell 106 (2001) 309–318.
[7] B. Wittig, S. Wolfl, T. Dorbic, W. Vahrson, A. Rich, Transcription of human c-*myc* in permeabilized nuclei is associated with formation of Z-DNA in three discrete regions of the gene, EMBO J. 11 (1992) 4653–4663.
[8] S. Wolfl, B. Wittig, A. Rich, Identification of transcriptionally induced Z-DNA segments in the human c-*myc* gene, Biochim. Biophys. Acta 1264 (1995) 294–302.
[9] A. Herbert, J. Alfken, Y.-G. Kim, I.S. Mian, K. Nishimoto, A. Rich, A Z-DNA binding domain present in the human editing enzyme, double-stranded RNA adenosine deaminase, Proc. Natl Acad. Sci. USA 94 (1997) 8421–8426.
[10] Y.-G. Kim, M. Muralinath, T. Brandt, M. Pearcy, K. Hauns, K. Lowenhaupt, B.L. Jacobs, A. Rich, A role for Z-DNA binding in vaccinia virus pathogenesis, Proc. Natl Acad. Sci. USA 100 (2003) 6974–6979.
[11] K. Lowenhaupt, B.-K. Oh, K.K. Kim, A. Rich, Evidence that vaccinia virulence factor E3L binds to Z-DNA in vivo: implications for development of a therapy for poxvirus infection, Proc. Natl Acad. Sci. USA 101 (2004) 1514–1518.
[12] J.A. Kwon, A. Rich, Biological function of the vaccinia virus Z-DNA-binding protein E3L: gene transactivation and antiapoptotic activity in HeLa cells, Proc. Natl Acad. Sci. USA 102 (2005) 12759–12764.
[13] T. Schwartz, J. Behike, K. Lowenhaupt, U. Heinemann, A. Rich, Structure of the DLM-1–Z-DNA complex reveals a conserved family of Z-DNA-binding proteins, Nat. Struct. Biol. 8 (2001) 761–765.
[14] Y.-G. Kim, K.-M. Thai, J. Song, K.K. Kim, H.-J. Park, Identification of novel ligands for the Z-DNA binding protein by structure-based virtual screening, Chem. Pharm. Bull. 55 (2007) 340–342.
[15] J.H. Riazance-Lawrence, W.C. Johnson Jr., Multivalent ions are necessary for poly[d(AC)·d(GT)] to assume the Z form: a CD study, Biopoly. 32 (1992) 271–276.
[16] H.S. Basu, H.C.A. Schwietert, B.G. Feuerstein, L.J. Marton, Effects of variation in the structure of spermine on the association with DNA and the induction of DNA conformational changes, Biochem. J. 269 (1990) 329–334.
[17] DNA and RNA structure, in: G.M. Blackburn, M.J. Gait (Eds.), Nucleic Acids in Chemistry and Biology, Oxford University Press, Oxford, 1996, pp. 15–81.
[18] M. Behe, G. Felsenfeld, Effects of methylation on a synthetic polynucleotide: the B–Z transition in poly(dG-m^5dC)·poly(dG-m^5dC), Proc. Natl Acad. Sci. USA 78 (1981) 1619–1623.
[19] A. Moller, A. Nordheim, S.A. Kozlowski, D.J. Patel, A. Rich, Bromination stabilizes poly(dG-dC) in the Z-DNA form under low-salt conditions, Biochem. 23 (1984) 54–62.
[20] Y. Xu, R. Ikeda, H. Sugiyama, 8-Methylguanosine: a powerful Z-DNA stabilizer, J. Am. Chem. Soc. 125 (2003) 13519–13524.
[21] H. Sugiyama, K. Kawai, A. Matsunaga, K. Fujimoto, I. Saito, H. Robinson, A.H.J. Wang, Synthesis, structure and thermodynamic properties of 8-methylguanine-containing oligonucleotides: Z-DNA under physiological salt conditions, Nucleic Acids Res. 24 (1996) 1272–1278.
[22] L.P.A. van Houte, J.G. Westra, R. van Grondelle, A spectroscopic study of the conformation of poly d(G-C).poly d(G-C) modified with the carcinogen 2-aminofluorene, Carcingenesis 9 (1988) 1017–1027.
[23] P. Abuaf, F.F. Kadlubar, D. Grunberger, Circular dichroism of poly(dG-dC) modified by the carcinogens N-methyl-4-aminoazobenzene or 4-aminobiphenyl, Nucleic Acids Res. 15 (1987) 7125–7136.
[24] P.M. Gannett, S. Heavner, J.R. Daft, K.H. Shaughnessy, J.D. Epperson, N.L. Greenbaum, Synthesis, properties, and NMR studies of a C8-phenylguanine modified oligonucleotide that preferentially adopts the Z-DNA conformation, Chem. Res. Toxicol. 16 (2003) 1385–1394.
[25] P.M. Gannett, T. Lawson, M. Miller, D.D. Thakkar, J.W. Lord, W.-M. Yau, B. Toth, 8-arylguanine adducts from arenediazonium ions and DNA, Chem. Biol. Interact. 95 (1996) 1–25.
[26] P.M. Gannett, X. Shi, J. Ye, J.H. Powell, E. Darian, J. Daft, Activation of AP-1 through the MAP kinase pathway: a potential mechanism of the carcinogenic effect of arenediazonium ions, Chem. Res. Toxicol. 13 (2000) 1020–1027.
[27] S. Heavner, P.M. Gannett, Molecular dynamics and free energy calculations of the B and Z forms of C8-arylguanine modified oligonucleotides, J. Biomol. Struct. Dyn. 23 (2005) 203–219.
[28] S.C. Ha, K. Lowenhaupt, A. Rich, Y.-G. Kim, K.K. Kim, Crystal structure of a junction between B-DNA and Z-DNA reveals two extruded bases, Nature 437 (2005) 1183–1186.
[29] V. Vongsutilers, P.M. Gannett, A general synthesis of C8-arylpurine phosphoramidites, Molecules 14 (2009) 3339–3352.
[30] L.E. Xodo, G. Manzini, F. Quadrifoglio, G.A. van der Marei, J.H. van Boom, The B–Z conformational transition in folded oligodeoxynucleotides: loop size and stability of Z-hairpins, Biochem. 27 (1988) 6327–6331.
[31] Z. Reich, P. Friedman, S. Levin-Zaidman, A. Minsky, Effects of adenine tracts on the B–Z transition, J. Biol. Chem. 268 (1993) 8261–8266.
[32] D.-M. Soumpasis, Statistical mechanics of the B → Z transition of DNA: contribution of diffuse ionic interactions, Proc. Natl Acad. Sci. USA 81 (1984) 5116–5120.
[33] M.J. Doktycz, A.S. Benight, R.D. Sheardy, Energetics of B–Z junction formation in a sixteen base-pair duplex DNA, J. Mol. Biol. 212 (1990) 3–6.
[34] R. Boelens, R.M. Scheek, K. Dijkstra, R. Kaptein, Sequential assignment of imino- and amino-proton resonances in ^{1}H NMR spectra of oligonucleotides by two-dimensional NMR spectroscopy. application to a *lac* operator fragment, J. Magn. Reson. 62 (1985) 378–386.
[35] C.K. Mitra, M.H. Sarma, R.H. Sarma, Left-handed deoxyribonucleic acid double helix in solution, Biochem. 20 (1981) 2036–2041.
[36] J. Feigon, A.H.J. Wang, G.A. van der Marei, J.H. van Boom, A. Rich, A one- and two-dimensional NMR study of the B to Z transition of $(m^5$dC-dG$)_2$ in methanolic solution, Nucleic Acids Res. 12 (1984) 1243–1263.
[37] W.D. Cornell, P. Cieplak, C.I. Bayly, I.R. Gould Jr., K.M. Merz, D.M. Ferguson, D.C. Spellmeyer, T. Fox, J.W. Caldwell, P.A. Kollman, A second generation force field for the simulation of proteins and nucleic acids, J. Am. Chem. Soc. 117 (1995) 5179–5197.
[38] W.D. Cornell, P. Cieplak, C.I. Bayly, I.R. Gould Jr., K.M. Merz, D.M. Ferguson, D.C. Spellmeyer, T. Fox, J.W. Caldwell, P.A. Kollman, A second generation force field for the simulation of proteins, nucleic acids, and organic molecules, J. Am. Chem. Soc. 117 (1999) 5179–5197.
[39] D.A. Case, T.A. Darden, T.E. Cheatham, III, C.L. Simmerling, J. Wang, R.E. Duke, R. Luo, M. Crowley, R.C.Walker, W. Zhang, K.M. Merz, B. Wang, S. Hayik, A. Roitberg, G. Seabra, I. Kolossvary, K.F. Wong, F. Paesani, J. Vanicek, X. Wu, S.R. Brozell, T. Steinbrecher, H. Gohlke, L. Yang, C. Tan, J. Mongan, V. Hornak, G. Cui, D.H. Mathews, M.G. Seetin, C. Sagui, V. Babin, P.A. Kollman, AMBER 10, University of California, San Francisco, 2008.
[40] C. Simmerling, R. Elber, J. Zhang, A. Pullman, OIL-view — a program for visualization of structure and dynamics of biomolecules and STO — a program for computing stochastic paths, Modeling of Biomolecular Structure and Mechanisms, Kluwer, Netherlands, 1995, pp. 241–265.
[41] R. Lavery, H. Sklenar, The definition of generalized helicoidal parameters and of axis curvature for irregular nucleic acids, J. Biomol. Struct. Dyn. 6 (1988) 63–91.
[42] R. Lavery, H. Sklenar, Defining the structures of irregular nucleic acids: conventions and principles, J. Biomol. Struct. Dyn. 6 (1988) 655–667.
[43] J.L. Sessler, M. Sathiosatham, K. Doerr, V. Lynch, K.A. Abboud, A G-quartet formed in the absence of a templating metal cation: a new 8-(N,N-dimethylaniline) guanosine derivative, Angew. Chem. Int. Ed. 39 (2000) 1300–1303.
[44] W.C. Johnson, CD of nucleic acids, in: N. Berova, K. Nakanishi, R.W. Woody (Eds.), Circular Dichroism: Principles and Applications, John Wiley & Sons, Inc, New York, NY, 2000, pp. 703–718.
[45] F.M. Pohl, T.M. Jovin, Salt-induced coperative conformational change of a synthetic DNA: equilibrium and kinetic studies with poly (dG-dC), J. Mol. Biol. 67 (1972) 375–396.
[46] P. Várnai, K. Zakrzewska, DNA and its counterions: a molecular dynamics study, Nucleic Acids Res. 32 (2004) 4269–4280.
[47] S.Y. Ponomarev, K.M. Thayer, D.L. Beveridge, Ion motions in molecular dynamics simulations on DNA, Proc. Natl Acad. Sci. USA 101 (2004).
[48] J. Petruska, M.F. Goodman, Enthalpy–entropy compensation in DNA melting thermodynamics, J. Biol. Chem. 270 (1995) 746–750.
[49] A.G. Herbert, A. Rich, A method to identify and characterize Z-DNA binding proteins using a linear oligodeoxynucleotide, Nucleic Acids Res. 21 (1993) 2669–2672.
[50] Y.-M. Kang, J. Bang, E.H. Lee, H.-C. Ahn, Y.-J. Seo, K.K. Kim, Y.-G. Kim, B.-S. Choi, J.-H. Lee, NMR spectroscopic elucidation of the B–Z transition of a DNA double helix induced by the Zα domain of human ADAR1, J. Am. Chem. Soc. 131 (2009) 11485–11491.
[51] E.H. Lee, Y.-J. Seo, H.-C. Ahn, Y.-M. Kang, H.-E. Kim, Y.-M. Lee, B.-S. Choi, J.-H. Lee, NMR study of hydrogen exchange during the B–Z transition of a DNA duplex induced by the Zα domains of yatapoxvirus E3L, FEBS Lett. 584 (2010) 4453–4457.